SERBIAN JOURNAL OF ELECTRICAL ENGINEERING
Vol. 16, No. 3, October 2019, 439-454

UDC: 621.316 **DOI: https://doi.org/10.2298/SJEE1903439K**

Time Domain Analysis of Excess Loss in Electrical Steel

Branko Koprivica[1], Marko Rosić[1], Krzysztof Chwastek[2]

Abstract: The aim of this paper is to present a comprehensive approach to analyse and interpret power loss in ferromagnetic materials with particular attention devoted to excess power loss. Experimental results obtained with an Epstein frame and toroidal core made of electrical steel are presented in the paper, including quasistatic and dynamic hysteresis loops. According to the time waveforms of the measured magnetic field and magnetic flux density, an instantaneous power loss is calculated for the quasistatic and dynamic case. Moreover, the instantaneous power loss due to eddy current is calculated, as well as the instantaneous excess power loss and excess magnetic field. This excess magnetic field is compared to the excess magnetic field calculated by Bertotti's model. Analysis and discussion of the results obtained is given in the paper.

Keywords: Time Domain, Power Loss, Excess Power Loss, Electrical Steel.

1 Introduction

Given that the actual waveforms of magnetic flux density in the electrical machines and transformers include higher harmonic flux densities [1], and that these machines can now be designed using numerical methods by applying harmonic analysis [2], it is very important to obtain a power loss model with high accuracy to increase their efficiency. This is currently a topic of interest for many researchers [3 – 12]. In addition, the magnetising conditions in electrical machines and transformers include rotational magnetic fields and magnetic fluxes [1, 13], so the power loss model should also be applicable in such cases.

A widely accepted model of power loss in ferromagnetic materials is presented in [14]. This model predicts three types of power loss: hysteresis loss, classical eddy current loss and excess (anomalous) loss. The model has been applied by many scientists and researchers [3 – 12]. The particular importance of this model lies in its comprehensive representation of excess loss and the introduction of so-called magnetic objects. However, the main concern

[1]University of Kragujevac, Faculty of Technical Sciences in Čačak, Svetog Save 65, 32000 Čačak, Serbia; E-mails: branko.koprivica@ftn.kg.ac.rs, marko.rosic@ftn.kg.ac.rs
[2]Czestochowa University of Technology, Faculty of Electrical Engineering, Armii Krajowej 17, 42-200 Czestochowa, Poland; E-mail: krzysztof.chwastek@gmail.com

regarding this model is its application in the analysis of average values of power loss (obtained by measurements), but not in the analysis of instantaneous power loss (can be calculated from measurements). On this basis, only quantitative information (numerical values) on power loss is obtained, while qualitative representation (time waveforms) is omitted.

The analysis presented in this paper is devoted to the calculation of instantaneous excess power loss in electrical steel. The calculations are performed with measurement results obtained with an Epstein frame for non-oriented steel and toroidal core for grain-oriented steel under quasistatic (frequency of 1 Hz) and dynamic (frequency of 50 Hz) conditions. Measurements are made under a controlled time waveform of magnetic flux density in the cases of sinusoidal and triangular shape. Time waveforms (instantaneous values) of the magnetic field and magnetic flux density are obtained and saved during the experiments. A PC based system with data acquisition cards and LabVIEW software is used for all measurements. Further calculations are also made using the LabVIEW software, independently from measurements.

The paper contains experimental and calculation results, as well as their detailed analysis and discussion.

2 Theoretical Approach of Three-Term Model

The concept of power loss separation into three terms was described in details by Bertotti in 1998 [14]. Theoretical considerations and a comprehensive analysis of experimental results are presented in [15, 16]. The basic idea of this concept is that the total instantaneous power loss $p_{tot}(t)$ in a soft ferromagnetic material can be separated into three components - hysteresis power loss $p_{hyst}(t)$, classical eddy current power loss $p_{cl}(t)$ and excess power loss $p_{exc}(t)$:

$$p_{tot}(t) = p_{hyst}(t) + p_{cl}(t) + p_{exc}(t) = H_{tot}(t)\frac{\mathrm{d}B(t)}{\mathrm{d}t} \quad \left[\frac{\mathrm{W}}{\mathrm{m}^3}\right], \tag{1}$$

where $H_{tot}(t)$ is the instantaneous total magnetic field and $B(t)$ is the instantaneous magnetic flux density of a dynamic hysteresis loop.

The first component of hysteresis power loss is related to the power loss obtained under a static magnetic field being applied or in the case of a quasistatic magnetic field being applied (frequency in the range of 1 Hz). This can be determined experimentally. The second component of classical eddy current loss can be calculated by applying analytical equations derived from the fundamental laws of electromagnetics (Maxwell equations and other constitutive relations) to the case of conductive material placed in the time-varying magnetic field. The third component of excess power loss is related to the domain wall motion (magnetic objects) under dynamic magnetic field

applied to the material. These three components and their corresponding magnetic fields (obtained by deriving power loss by the rate of magnetic flux density d$B(t)$/dt) are described as follows:

$$p_{hyst}(t) = H_{hyst}(t)\frac{\mathrm{d}B(t)}{\mathrm{d}t}\left[\frac{\mathrm{W}}{\mathrm{m}^3}\right],\ H_{hyst}(t) \text{ - measured}, \tag{2}$$

$$p_{cl}(t) = H_{cl}(t)\frac{\mathrm{d}B(t)}{\mathrm{d}t}\left[\frac{\mathrm{W}}{\mathrm{m}^3}\right],\ H_{cl}(t) = \frac{\sigma d^2}{12}\frac{\mathrm{d}B(t)}{\mathrm{d}t}\left[\frac{\mathrm{A}}{\mathrm{m}}\right], \tag{3}$$

$$p_{exc}(t) = H_{exc}(t)\frac{\mathrm{d}B(t)}{\mathrm{d}t}\left[\frac{\mathrm{W}}{\mathrm{m}^3}\right], H_{excB}(t) = \frac{n_0 V_0}{2}\left(\sqrt{1+\frac{4\sigma GS}{n_0^2 V_0}\frac{\mathrm{d}B(t)}{\mathrm{d}t}}-1\right)\left[\frac{\mathrm{A}}{\mathrm{m}}\right], \tag{4}$$

where σ is the conductivity of the material, d is the thickness of the material (in the case of the laminated material such as electrical steel), $H_{hyst}(t)$ is the instantaneous magnetic field obtained under quasistatic conditions, $H_{cl}(t)$ is the instantaneous magnetic field of the classical eddy current, $H_{exc}(t)$ is the instantaneous excess magnetic field, $H_{excB}(t)$ is the instantaneous excess magnetic field derived by Bertotti, G is a coefficient equal to 0.1356, S is the cross-section area of the sample and n_0 and V_0 are phenomenological parameters characterising a given material. Expression for $H_{excB}(t)$ in (4) is derived under the assumption that the effective number of active magnetic objects n is linearly proportional to the excess field $H_{exc}(t)$ [14]:

$$n = n_0 + \frac{H_{exc}(t)}{V_0}. \tag{5}$$

Parameters n_0 and V_0 need to be determined from the measurement of static (quasistatic) and dynamic hysteresis loops (power loss) and obtained values can be further used for calculation of power loss under various magnetising conditions.

This approach has been widely accepted by scientists and engineers and it has been applied more or less successfully under various magnetising conditions [3 – 12], such as: variable amplitude and frequency of the applied magnetic field, different shapes of the magnetic field or the magnetic flux density, under axial or rotational magnetising field and many others of interest. By following the recommendations given in international standard IEC 60404-2 [17], the total power loss should be measured under the sinusoidal waveform of magnetic flux density. Parameters n_0 and V_0 are most often calculated using these measurement results, with average values of power loss and effective values of magnetic field and magnetic flux density. Further calculations are usually performed to predict the total power loss at different conditions of interest. Deviations between calculated and measured total power loss can exceed several percent [5].

The deviation increases if the magnetising conditions are complex (higher harmonics or DC component) and it can reach several tens of percent [18]. Such conditions (higher harmonic components) have been analysed in the technical report IEC TR 62383 [18]. By taking into consideration that parameter V_0 depends on the magnetic flux density and by applying improvements in the calculations, the deviations reported are kept below 5%. This seems acceptable, but lower deviations are needed in high-fidelity calculations and simulations. It should be taken into consideration that the improvements in the energy efficiency of electrical machines and transformers are in the range of a few percent or less and that the prediction of power loss with such a high deviation is not appropriate.

It has been already shown that (5) is not valid in all cases, for all magnetic materials [19]. Therefore, a more comprehensive analysis of the three-term power loss model should be performed in order to identify the causes of the deviation. An approach to such an analysis is given in the following section.

3 Proposed Approach

In the proposed approach, the three-term model of power loss in ferromagnetic material (electrical steel) has been applied in a more comprehensive manner in order to increase the quality of the analysis. For this purpose, all the calculations should be performed with instantaneous values of magnetic field and magnetic flux density (actually with corresponding numerical values) obtained from measurements and calculations. Special attention needs to be devoted to the calculation of instantaneous excess power loss, as the most specific component of power loss.

According to (1), $p_{exc}(t)$ can be calculated by:

$$p_{exc}(t) = p_{tot}(t) - p_{hyst}(t) - p_{cl}(t) \left[\frac{\mathrm{W}}{\mathrm{m}^3}\right]. \tag{6}$$

Instantaneous $p_{tot}(t)$ given by (1) should be calculated using $H_{tot}(t)$ and $B(t)$ obtained from the measurement of the dynamic hysteresis loop, $p_{hyst}(t)$ given by (2) should be calculated using $H_{hyst}(t)$ obtained from the measurement of the quasistatic hysteresis loop and $B(t)$ obtained from the measurement of the dynamic hysteresis loop and $p_{cl}(t)$ should be calculated by (3), as well as $H_{cl}(t)$, using $B(t)$ obtained from the measurement of the dynamic hysteresis loop. Furthermore, $H_{exc}(t)$ can be calculated by:

$$H_{exc}(t) = \frac{p_{tot}(t) - p_{hyst}(t) - p_{cl}(t)}{\mathrm{d}B(t)/\mathrm{d}t} \left[\frac{\mathrm{A}}{\mathrm{m}}\right]. \tag{7}$$

To illustrate the approach, waveforms of measured $H_{tot}(t)$, $H_{hyst}(t)$ and $B(t)$ are presented in Fig. 1a and the corresponding quasistatic and dynamic hysteresis

loops are presented in Fig. 1b. Waveforms of power loss, total and all three components, calculated for the results given in Fig. 1, are presented in Fig. 2.

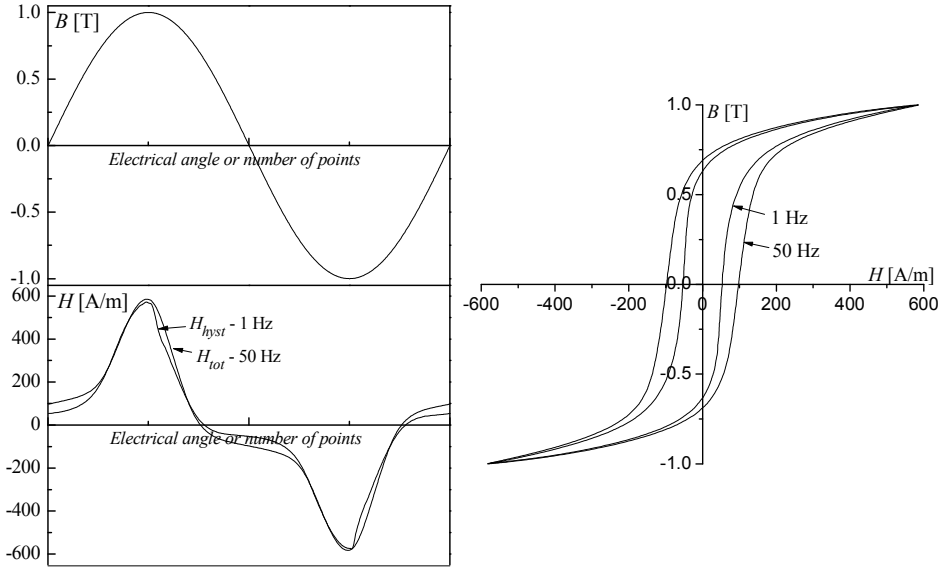

Fig. 1 – *Experimental results at* B_{max}= 1.0 T *for* 1 Hz *and* 50 Hz*:* (a) *waveforms of* $H_{tot}(t)$ *and* $H_{hyst}(t)$ *for sinusoidal* $B(t)$*;* (b) *corresponding hysteresis loops.*

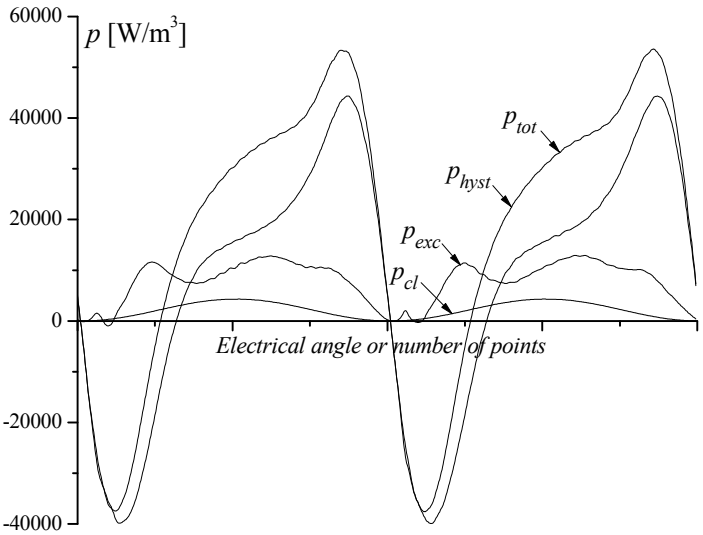

Fig. 2 – *Calculated waveforms of power loss for waveforms from Fig. 1.*

4 Results and Analysis

This section contains experimental results of interest, such as:

1) measured waveforms of magnetic field and magnetic flux density at B_{max} equal to 0.5 T, 1.0 T and 1.5 T, at frequencies of 1 Hz and 50 Hz, for sinusoidal and triangular $B(t)$, obtained with an Epstein frame for non-oriented electrical steel;
2) measured waveforms of magnetic field and magnetic flux density at B_{max} equal to 0.5 T, 1.0 T and 1.5 T, at frequencies of 1 Hz and 50 Hz, for sinusoidal and triangular $B(t)$, obtained with toroidal core for grain-oriented electrical steel;
3) corresponding quasistatic and dynamic hysteresis loops for all cases.

Also, this section contains calculation results of interest, such as:

1) corresponding waveforms of $p_{tot}(t)$ and $p_{hyst}(t)$ for all cases;
2) calculated waveforms of $p_{cl}(t)$ and $p_{exc}(t)$ for all cases;
3) calculated waveforms of $H_{exc}(t)$ for all cases;
4) corresponding hysteresis loops of excess power loss for all cases.

4.1 Non-oriented electrical steel

Figure 3 presents measured waveforms of $H_{tot}(t)$ (obtained at 50 Hz) and $H_{hyst}(t)$ (obtained at 1 Hz) for non-oriented steel at B_{max} equal to 0.5 T, 1.0 T and 1.5 T, when $B(t)$ is sinusoidal (Fig. 3a) or triangular (Fig. 3b).

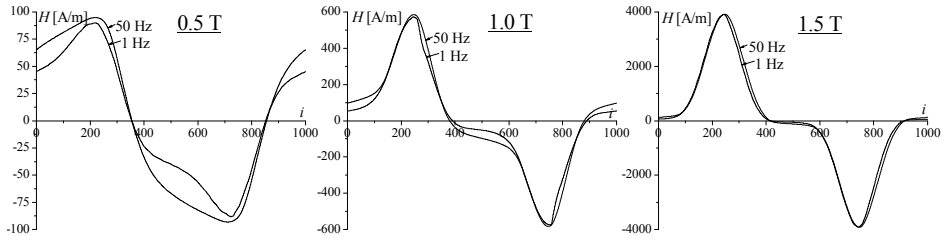

(a)

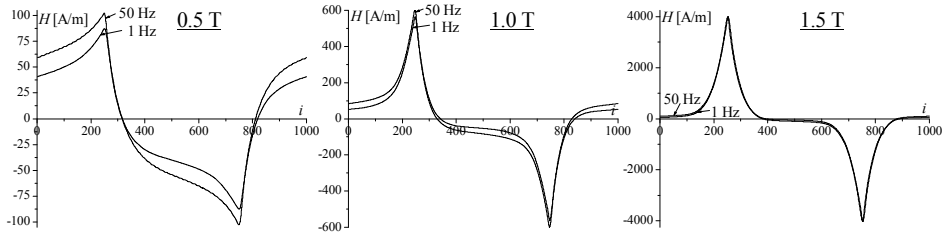

(b)

Fig. 3 – *Waveforms of* $H_{tot}(t)$ (50 Hz) *and* $H_{hyst}(t)$ (1 Hz) *for non-oriented steel when magnetic flux density is:* (a) *sinusoidal and* (b) *triangular.*

The corresponding hysteresis loops are presented in Fig. 4.

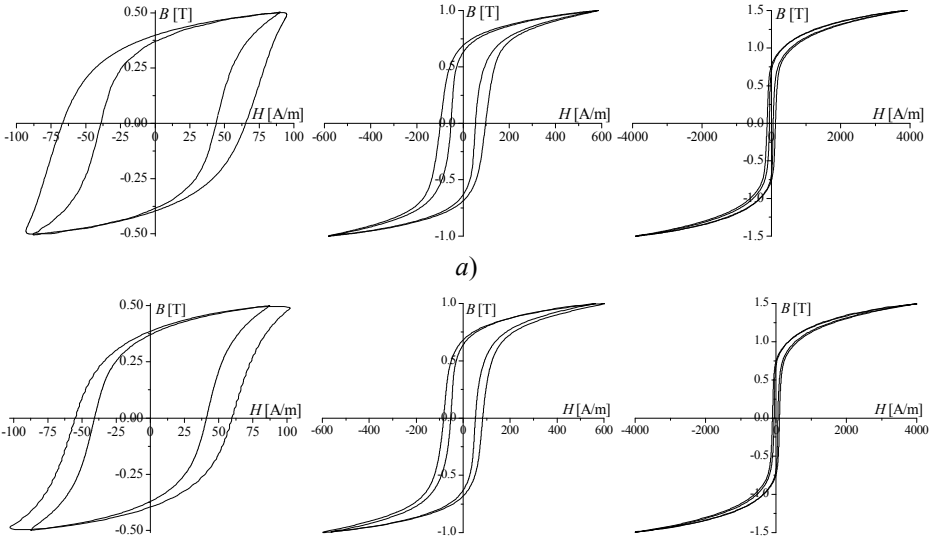

Fig. 4 – *Hysteresis loops at* 50 Hz *and* 1 Hz *for non-oriented steel when magnetic flux density is:* (a) *sinusoidal and* (b) *triangular.*

Total and hysteresis power loss calculated for waveforms from Fig. 3 are presented in Fig. 5.

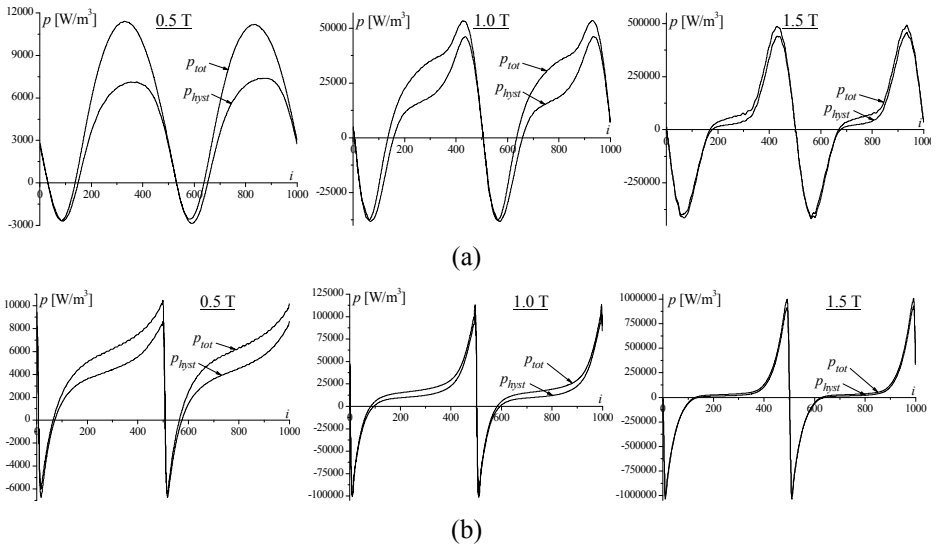

Fig. 5 – *Total loss at* 50 Hz *and hysteresis loss at* 1 Hz *for non-oriented steel when magnetic flux density is:* (a) *sinusoidal and* (b) *triangular.*

Classical eddy current and excess power loss calculated for waveforms from Fig. 3 are presented in Fig. 6.

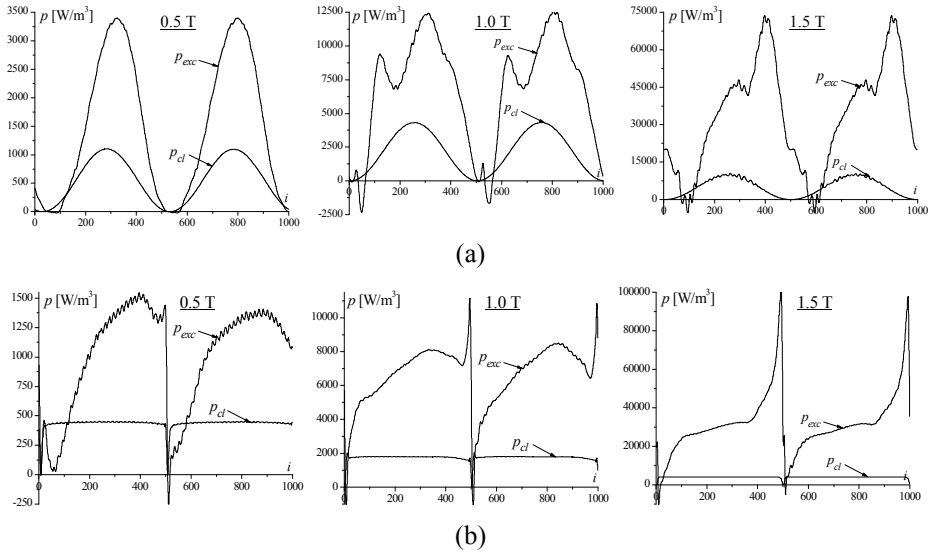

Fig. 6 – *Classical eddy current and excess loss for non-oriented steel when magnetic flux density is:* (a) *sinusoidal and* (b) *triangular.*

Excess magnetic field calculated for waveforms from Fig. 3 are presented in Fig. 7.

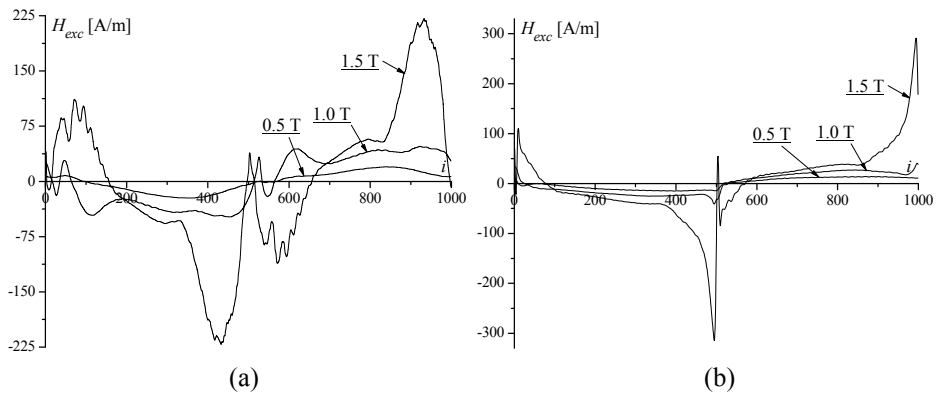

Fig. 7 – *Excess magnetic field for non-oriented steel when magnetic flux density is:* (a) *sinusoidal and* (b) *triangular.*

Hysteresis loops of excess loss for waveforms from Fig. 7 are presented in Fig. 8.

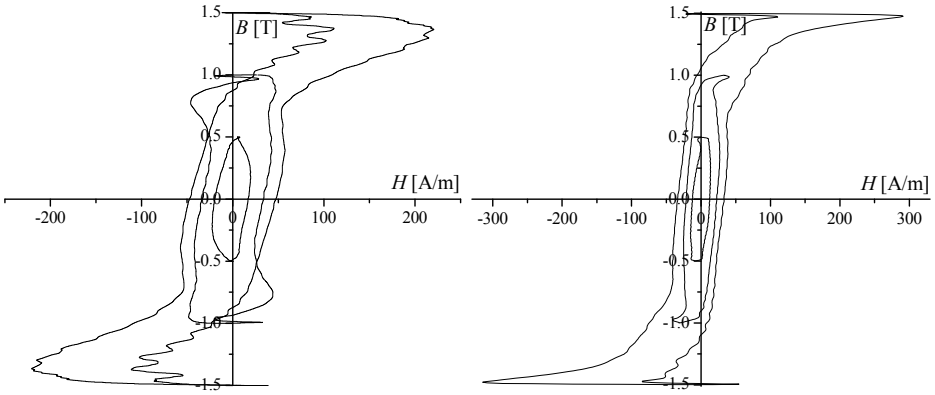

Fig. 8 – *Hysteresis loops of excess loss for non-oriented steel when magnetic flux density is:* (a) *sinusoidal and* (b) *triangular.*

4.2 Grain-oriented electrical steel

Figure 9 presents measured waveforms of $H_{tot}(t)$ (obtained at 50 Hz) and $H_{hyst}(t)$ (obtained at 1 Hz) for grain-oriented steel at B_{max} equal to 0.5 T, 1.0 T and 1.5 T, when $B(t)$ is sinusoidal (Fig. 9a) or triangular (Fig. 9b).

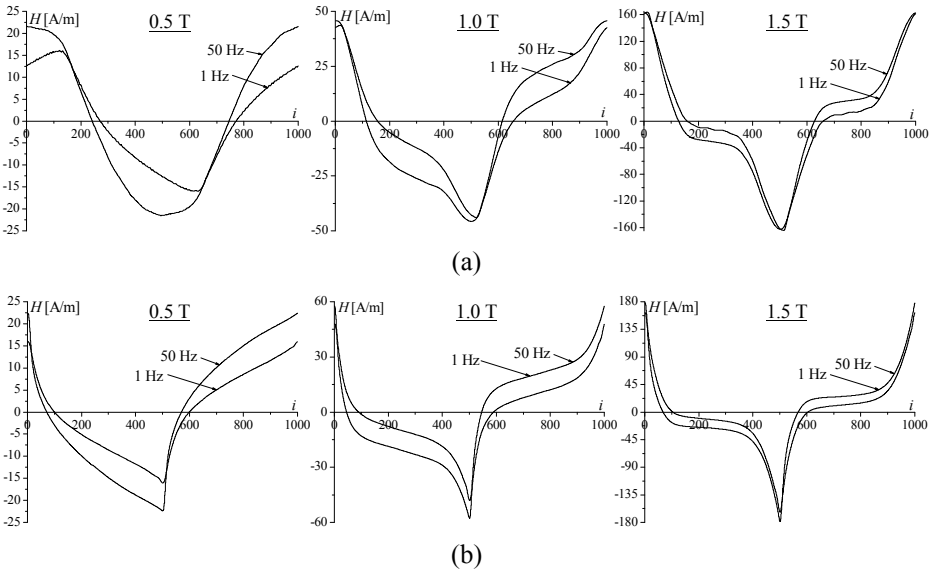

Fig. 9 – *Waveforms of* $H_{tot}(t)$ (50 Hz) *and* $H_{hyst}(t)$ (1 Hz) *for grain-oriented steel when magnetic flux density is:* (a) *sinusoidal and* (b) *triangular.*

The corresponding hysteresis loops are presented in Fig. 10.

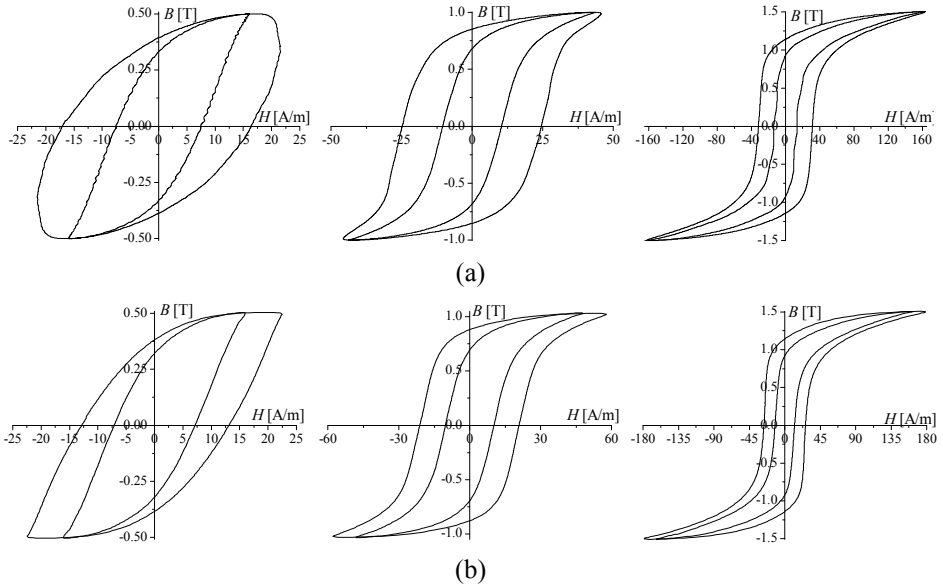

Fig. 10 – *Hysteresis loops at* 50 Hz *and* 1 Hz *for grain-oriented steel when magnetic flux density is:* (a) *sinusoidal and* (b) *triangular.*

Total and hysteresis power loss calculated for waveforms from Fig. 9 are presented in Fig. 11.

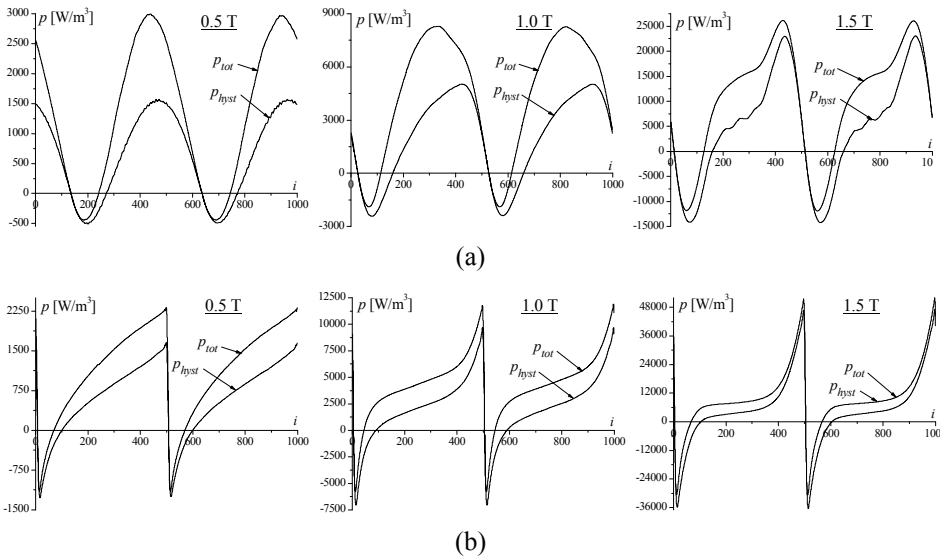

Fig. 11 – *Total loss at* 50 Hz *and hysteresis loss at* 1 Hz *for grain-oriented steel when magnetic flux density is:* (a) *sinusoidal and* (b) *triangular.*

Classical eddy current and excess power loss calculated for waveforms from Fig. 9 are presented in Fig. 12.

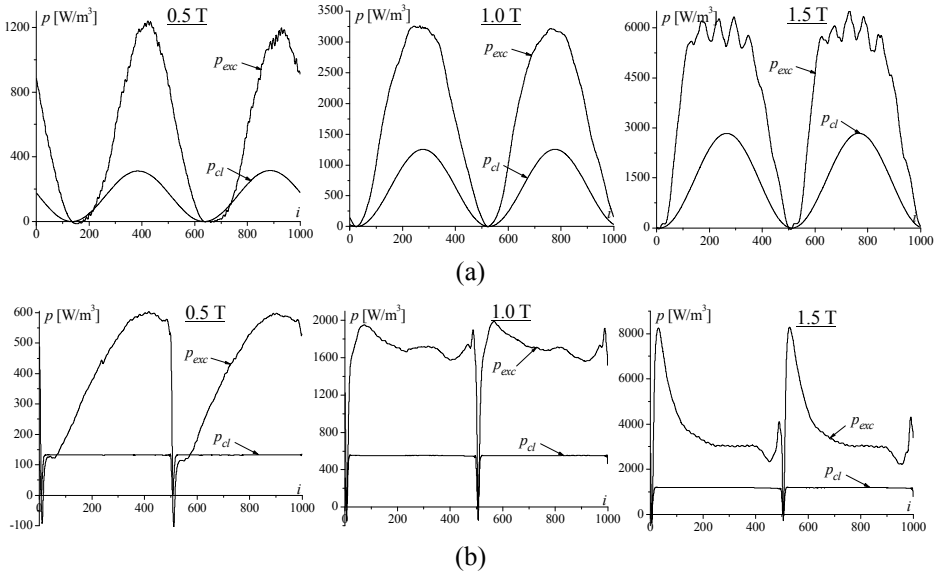

Fig. 12 – *Classical eddy current and excess loss for grain-oriented steel when magnetic flux density is:* (a) *sinusoidal and* (b) *triangular.*

Excess magnetic field calculated for waveforms from Fig. 9 are presented in Fig. 13.

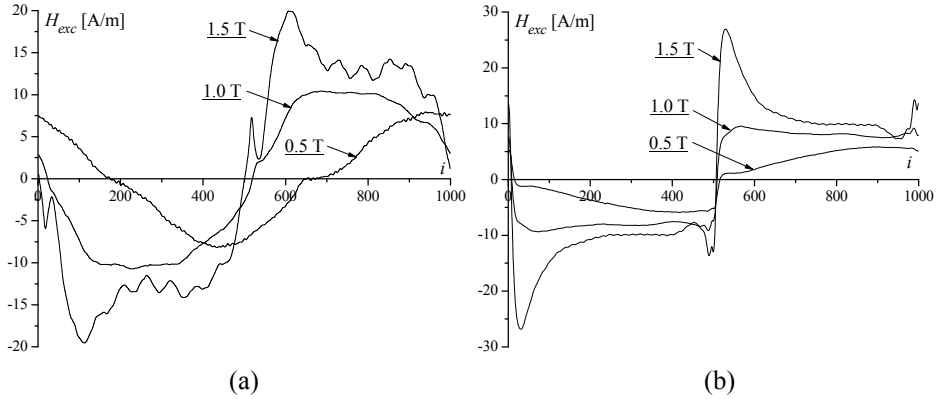

Fig. 13 – *Excess magnetic field for grain-oriented steel when magnetic flux density is:* (a) *sinusoidal and* (b) *triangular.*

Hysteresis loops of excess loss for waveforms from Fig. 13 are presented in Fig. 14.

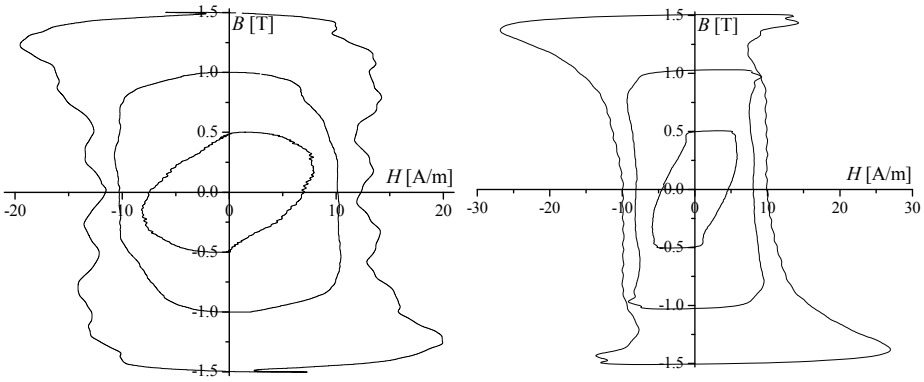

Fig. 14 – *Hysteresis loops of excess loss for grain-oriented steel when magnetic flux density is:* (a) *sinusoidal and* (b) *triangular.*

4.3 Analysis of results

The results given in Sections 4.1 and 4.2 were obtained using a comprehensive method for the analysis of power losses in ferromagnetic material, in this case in electrical steels. Several conditions in experiments and analysis need to be fulfilled to have the results measured, interpreted and evaluated correctly. These are:

1. waveforms of $H_{tot}(t)$, $H_{hyst}(t)$ and $B(t)$ need to be measured with the same number of samples per period because of requirements of numerical calculation;
2. correctness (precision) of measured waveforms of $H_{tot}(t)$, $H_{hyst}(t)$ and $B(t)$ is crucial from two aspects - first is related to the shape of the waveforms and second is related to amplitudes of waveforms;
3. alignment of two sets of waveforms measured independently, quasistatic and dynamic.

All waveforms presented in the paper consist of 1000 samples (numerical values - data points). Numerical calculations have been performed so that each i-th data point in one waveform is added (or any other operation) to i-th data point in another waveform.

Waveforms of $H_{tot}(t)$, $H_{hyst}(t)$ and $B(t)$ need to be measured without oscillations in order to minimise further deviation that may appear in the calculated waveforms. Such deviation can be observed in Fig. 9a for 1.5 T where $H_{hyst}(t)$ contains slight oscillations and in Figs. 12a and 13a where significant oscillations appear in calculated excess power loss and excess magnetic field. In addition, these oscillations can be observed on corresponding hysteresis loop presented in Fig. 14a. In the particular case, reason for such

deviation lies in difficulties in controlling of the highly distorted signal of low frequency. Furthermore, high precision needs to be achieved regarding the amplitudes of $H_{tot}(t)$, $H_{hyst}(t)$ and $B(t)$, especially of $B(t)$. It has been noticed that even small deviation of $B_{\max}$ between quasistatic and dynamic measurement (up to 1%) can introduce significant deviation in calculated waveforms. This is more expressed at higher $B_{\max}$. As it can be seen in Fig. 8a, large deviation exists in loops for excess loss at $B_{\max}$ equal to 1.0 T and 1.5 T, where unnatural deviation can be observed as loop approaches the maximum (minimum). The loop from Fig. 8a obtained at 1.5 T is additionally deformed because of oscillations in corresponding $H_{tot}(t)$ and $H_{hyst}(t)$ (Fig. 5a). Loop from Fig. 8b obtained at 1.5 T also shows significant deviation close to the maximum. Therefore, differences in $B_{\max}$ for quasistatic and dynamic measurements should be much lower than 1 %, to the third decimal place.

Waveforms of $H_{tot}(t)$, $H_{hyst}(t)$ and $B(t)$ have been obtained from two independent measurements, quasistatic and dynamic. Also, $p_{tot}(t)$, $p_{hyst}(t)$ and $p_{cl}(t)$ have been obtained through separate calculations. Further calculations use waveforms of $p_{tot}(t)$, $p_{hyst}(t)$ and $p_{cl}(t)$ together for obtaining of $p_{exc}(t)$. In this last step, waveforms of $p_{tot}(t)$ and $p_{cl}(t)$ are properly aligned (they come from dynamic measurement), while $p_{hyst}(t)$ need to be aligned properly with $p_{tot}(t)$. It has been found that decreasing parts of $p_{tot}(t)$ and $p_{hyst}(t)$ need to be aligned together so that these two waveforms simultaneously passing through zero, as it has been presented in Figs. 2, 5 and 10. This will ensure that the $p_{exc}(t)$ waveform is always positive (sometimes calculations return negative values, but in acceptably small part of the waveform, Fig. 6a).

Therefore, in addition to the power loss calculation, the analysis presented is also useful for evaluation of the quality of the measurement results.

The most important results among all results presented are those given in Figs. 6–8 and Figs. 12–14, which concern excess magnetic field and power loss.

Waveforms of $H_{exc}(t)$ presented in Figs. 7 and 13 clearly show that excess magnetic field cannot be accurately enough represented with $H_{excB}(t)$ given by (4). Because of much smaller intensity of the magnetic field measured, the quality of the waveforms presented is much better for grain-oriented steel and further analysis refers to these results, but it can be also applied similarly to the results for non-oriented steel. By fitting measured $H_{exc}(t)$ to $H_{excB}(t)$ it has been calculated that phenomenological parameters are: $n_0 = 20$ and $V_0 = 0.08$ A/m. Comparisons of calculated waveforms of $H_{exc}(t)$ and $H_{excB}(t)$ in the case of sinusoidal and triangular magnetic flux density are presented in Fig. 15 (only positive parts are given since (4) is valid only for positive $\mathrm{d}B(t)/\mathrm{d}t$). It can be observed from this figure that relatively good agreement of $H_{exc}(t)$ and $H_{excB}(t)$ exists for 1.0 T, while for 0.5 T and 1.5 T the difference is significant. Observed deviations are similar for both shapes of $B(t)$ which indicates that some

regularity exists. This should be investigated thoroughly in additional analysis. It might be reasonable to perform time domain analysis with results obtained under triangular $B(t)$. As discussed previously, the quality of experimental results under such conditions is better (lower oscillations at higher B_{max} and easier shape control). In addition, initial relations between power loss under sinusoidal and triangular shapes of $B(t)$ already exist in the literature [20 – 22].

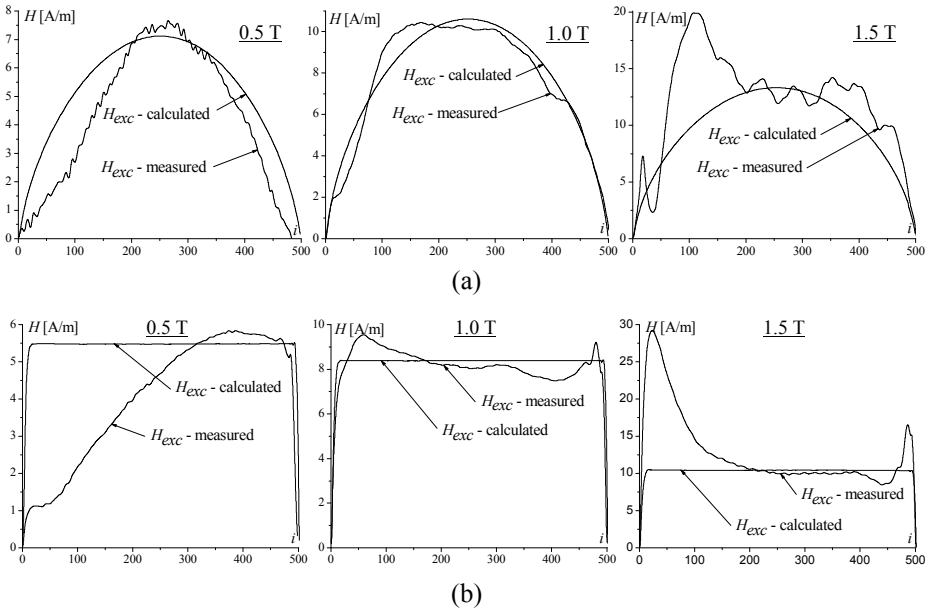

Fig. 15 – *Comparison of calculated* excess *magnetic fields for grain-oriented steel, when magnetic flux density is:* (a) *sinusoidal and* (b) *triangular.*

Future work may also be devoted to the possible physical explanation for the unusual shapes of hysteresis loops of excess loss shown in Fig. 14, especially those for B_{max}=1.5 T. The effect of loop deviation close to the maximum (minimum) might be related to experimental work of Hellmiss and Storm about the movement of an individual Bloch wall in a single-crystal picture frame of silicon iron [23].

5 Conclusion

Making high-fidelity measurements of magnetic characteristics of materials and creating comprehensive models of these characteristics lead to the better design and production of magnetic cores in electrical machines, transformers and components, which result in the increase of their efficiency, the improvement of control algorithms, the improvement of their performances, a decrease of noise and a decrease of the costs.

This paper presents a comprehensive analysis of power loss in non-oriented and grain-oriented electrical steel with emphasis to excess power loss analysis. This analysis is based on three-term model of power loss proposed by Bertotti. Different from other works, all calculations have been performed with measured instantaneous magnetic field and magnetic flux density (their waveforms). The analysis has been performed with experimental results obtained with Epstein frame and toroidal core under quasistatic (1 Hz) and dynamic (50 Hz) conditions, at maximal magnetic flux densities of 0.5 T, 1.0 T and 1.5 T. Time waveforms of magnetic fields and flux densities (corresponding hysteresis loops) have been recorded during the experiment, in the case of sinusoidal and triangular shape of magnetic flux density. An instantaneous hysteresis power loss for quasistatic case and instantaneous total power loss for dynamic case have been calculated. Also, instantaneous excess power loss and instantaneous excess magnetic field have been calculated. The obtained excess field has been compared to the excess field calculated by Bertotti's model.

The analysis and discussion of all results presented are given in the paper. Most importantly, it has been found that significant difference exists between excess magnetic fields calculated by proposed and Bertotti's methods at lower and higher magnetic flux densities (0.5 T and 1.5 T), while the difference is much lower at medium flux density of 1 T. Similar differences have been observed for sinusoidal and triangular case, which indicates that some rule exists.

The presented analysis supports the idea that a better model is needed for the calculation of excess power loss and excess magnetic field.

6 References

[1] S.J. Chapman: Electric Machinery Fundamentals, McGraw-Hill, NY, USA, 2005.

[2] https://www.comsol.com/.

[3] T. Matsuo, M. Shimasaki: Simple Modeling of the AC Hysteretic Property of a Grain-Oriented Silicon Steel Sheet, IEEE Transactions on Magnetics, Vol. 42, No. 4, April 2006, pp. 919 – 922.

[4] W.A. Roshen: A Practical, Accurate and Very General Core Loss Model for Nonsinusoidal Waveforms, IEEE Transactions on Power Electronics, Vol. 22, No. 1, January 2007, pp. 30 – 40.

[5] W.A. Pluta: Core Loss Models in Electrical Steel Sheets with Different Orientation, Przegląd Elektrotechniczny (Electrical Review), Vol. 87, No. 9b, September 2011, pp. 37 – 42.

[6] Y. Gao, Y. Matsuo, K. Muramatsu: Investigation on Simple Numeric Modeling of Anomalous Eddy Current Loss in Steel Plate Using Modified Conductivity, IEEE Transactions on Magnetics, Vol. 48, No. 2, February 2012, pp. 635 – 638.

[7] H. Zhao, C. Ragusa, O. de la Barrière, M. Khan, C. Appino, F. Fiorillo: Magnetic Loss Versus Frequency in Non-Oriented Steel Sheets and Its Prediction: Minor Loops, PWM, and the Limits of the Analytical Approach, IEEE Transactions on Magnetics, Vol. 53, No. 11, Nov. 2017, p. 2003804.

[8] S. Yue, Q. Yang, Y. Li, C. Zhang: Core Loss Calculation for Magnetic Materials Employed in SMPS under Rectangular Voltage Excitations, AIP Advances, Vol. 8, No. 5, January 2018, p. 056121.

[9] M. Dems, K. Komeza, J. Szulakowski, W. Kubiak: Modeling of Core Loss for Non-oriented Electrical Steel, COMPEL - The International Journal for Computation and Mathematics in Electrical and Electronic Engineering, Published Online in November 2018.

[10] P. Rasilo, W. Martinez, K. Fujisaki, J. Kyyra, A. Ruderman: Simulink Model for PWM-Supplied Laminated Magnetic Cores Including Hysteresis, Eddy-Current, and Excess Losses, IEEE Transactions on Power Electronics, Vol. 34, No. 2, February 2019, pp. 1683 – 1695.

[11] B. Schauerte, S. Steentjes, A. Thul, K. Hameyer: Advanced Iron-loss Estimation for Arbitrary Magnetization Loci in Non-oriented Electrical Steel Considering Anisotropic Effects, International Journal of Applied Electromagnetics and Mechanics, Vol. 61, No. S1, 2019, pp. S89 – S96.

[12] O. de la Barrière, C. Ragusa, C. Appino, F. Fiorillo: Loss Prediction in DC-Biased Magnetic Sheets, IEEE Transactions on Magnetics, Vol. 55, No. 10, Oct. 2019, p. 2002614.

[13] G. Shilyashki, H. Pfützner, E. Gerstbauer, G. Trenner, P. Hamberger, M. Aigner: Numerical Prediction of Rhombic Rotational Magnetization Patterns in a Transformer Core Package, IEEE Transactions on Magnetics, Vol. 52, No. 1, January 2016, p. 7200110.

[14] G. Bertotti: Hysteresis in Magnetism - For Physicists, Materials Scientists, and Engineers, Academic Press, San Diego, CA, USA, 1998.

[15] G. Bertotti: Physical interpretation of eddy current losses in ferromagnetic materials - I - Theoretical considerations, Journal of Applied Physics, Vol. 57, No. 6, March 1985, pp. 2110 – 2117.

[16] G. Bertotti: Physical interpretation of eddy current losses in ferromagnetic materials - II - Analysis of Experimental Results, Journal of Applied Physics, Vol. 57, No. 6, March 1985, pp. 2118 – 2126.

[17] IEC 60404-2 Ed. 3.1: Magnetic Materials: Part 2: Methods of Measurement of the Magnetic Properties of Electrical Steel Strip and Sheet by Means of an Epstein Frame, Geneva, Switzerland, June 2008.

[18] IEC TR 62383 Ed. 1.0: Determination of Magnetic Loss under Magnetic Polarization Waveforms including Higher Harmonic Components - Measurement, Modelling and Calculation Methods, Geneva, Switzerland, January 2006.

[19] G. Bertotti: General Properties of Power Losses in Soft Ferromagnetic Materials, IEEE Transactions on Magnetics, Vol. 24, No. 1, January1988, pp. 621 – 630.

[20] T. Sato, Y. Sakaki: Discussion on Eddy Current Loss under Square Wave Voltage Excitation, IEEE Transactions on Magnetics, Vol. 24, No. 6, November 1988, pp. 2904 – 2906.

[21] A.J. Moses, J. Leicht: Power Loss of Non Oriented Electrical Steel Under Square Wave Excitation, IEEE Transactions on Magnetics, Vol. 37, No. 4, July 2001, pp. 2737 – 2739.

[22] H. Zhao, C. Ragusa, C. Appino, O. de la Barrière, Y. Wang, F. Fiorillo: Energy Losses in Soft Magnetic Materials under Symmetric and Asymmetric Induction Waveforms, IEEE Transactions on Power Electronics, Vol. 34, No. 3, March 2019, pp. 2655 – 2665.

[23] G. Hellmiss, L. Storm: Movement of an Individual Bloch Wall in a Single-Crystal Picture Frame of Silicon Iron at Very Low Velocities, IEEE Transactions on Magnetics, Vol. 10, No. 1, March 1974, pp. 36 – 38.